

Pressure in active matter

Guo Yu(余果), Ruiyao Li(李蕤耀), Fukang Li(李富康), Jiayu Zhang(张佳玉), Xiyue Li(李西月), Zequ Chen(陈泽渠), Joscha Mecke, and Yongxiang Gao(高永祥)

Citatio: Chin. Phys. B, 2025, 34 (**9**): 094702. DOI: 10.1088/1674-1056/ae030c
http://cpb.iphy.ac.cn; http://iopscience.iop.org/cpb

What follows is a list of articles you may be interested in

On the spreading behavior of a droplet on a circular cylinder using the lattice Boltzmann method

Fan Yang(杨帆), Hu Jin(金虎), and Mengyao Dai(戴梦瑶)
Chin. Phys. B, 2024, 33 (**6**): 064702. DOI: 10.1088/1674-1056/ad3b7f

Active thermophoresis and diffusiophoresis

Huan Liang(梁欢), Peng Liu(刘鹏), Fangfu Ye(叶方富), and Mingcheng Yang(杨明成)
Chin. Phys. B, 2022, 31 (**10**): 104702. DOI: 10.1088/1674-1056/ac754d

Investigation of cavitation bubble collapse in hydrophobic concave using the pseudopotential multi-relaxation-time lattice Boltzmann method

Minglei Shan(单鸣雷), Yu Yang(杨雨), Xuemeng Zhao(赵雪梦), Qingbang Han(韩庆邦), and Cheng Yao(姚澄)
Chin. Phys. B, 2021, 30 (**4**): 044701. DOI: 10.1088/1674-1056/abcf4b

Simulation of microswimmer hydrodynamics with multiparticle collision dynamics

Andreas Z?ttl
Chin. Phys. B, 2020, 29 (**7**): 074701. DOI: 10.1088/1674-1056/ab943f

Lattice Boltzmann simulation of liquid–vapor system by incorporating a surface tension term

Song Bao-Wei (宋保维), Ren Feng (任峰), Hu Hai-Bao (胡海豹), Huang Qiao-Gao (黄桥高)
Chin. Phys. B, 2015, 24 (**1**): 014703. DOI: 10.1088/1674-1056/24/1/014703

INVITED REVIEW

Pressure in active matter

Guo Yu(余果)[1], Ruiyao Li(李蕤耀)[1], Fukang Li(李富康)[1], Jiayu Zhang(张佳玉)[1], Xiyue Li(李西月)[1], Zequ Chen(陈泽渠)[1], Joscha Mecke[1,2,†], and Yongxiang Gao(高永祥)[1,‡]

[1] *Institute for Advanced Study, Shenzhen University, Shenzhen* 518060, *China*

[2] *College of Physics and Optoelectronic Engineering, Shenzhen University, Shenzhen* 518060, *China*

(Received 13 August 2025; revised manuscript received 27 August 2025; accepted manuscript online 4 September 2025)

In the last decade, the study of pressure in active matter has attracted growing attention due to its fundamental relevance to nonequilibrium statistical physics. Active matter systems are composed of particles that consume energy to sustain persistent motion, which are inherently far from equilibrium. These particles can exhibit complex behaviors, including motility-induced phase separation, clustering, and anomalous stress distributions, motivating the introduction of active swim stress and swim pressure. Unlike in passive fluids, pressure in active systems emerges from momentum flux originating from swim force rather than equilibrium conservative interactions, offering a distinct perspective for understanding their mechanical response. Simple models of active Brownian particles (ABPs) have been employed in theoretical and simulation studies across both dilute and dense regimes, revealing that pressure is a state function and exhibits a nontrivial dependence on density. Together with nonequilibrium statistical concepts such as effective temperature and effective adhesion, pressure offers important insight for understanding behaviors in active matter such as sedimentation equilibrium and motility induced phase separation. Extensions of ABP models beyond their simplest form have underscored the fragility of the pressure-based equation of state, which can break down under factors such as density-dependent velocity, torque, complex boundary geometries and interactions. Building on these developments, this review provides a comprehensive survey of theoretical and experimental advances, with particular emphasis on the microscopic origins of active pressure and the mechanisms underlying the breakdown of the equation of state.

Keywords: active matter, active pressure, equation of state, active Brownian particles

PACS: 47.57.jd, 05.70.Ln, 47.63.Gd, 05.70.Ce

DOI: 10.1088/1674-1056/ae030c **CSTR:** 32038.14.CPB.ae030c

1. Introduction

Over the past two decades, active matter has gained widespread prominence across disciplines such as colloid science,[1,2] condensed matter physics,[3,4] nonequilibrium thermodynamics,[5,6] and self-assembly.[7–9] When a system's components consume energy from the environment to generate forces and remain in a nonequilibrium state, it is referred to as an active matter system.[10–12] Active matter offers a paradigm for numerous driven systems within the realm of soft and living matter, including biological systems such as bacterial colonies,[13] tissues and cells,[14] flocks of birds,[15] schools of fish,[16–18] bee colonies,[19,20] crowds of human beings,[21] and synthesized active matter consisting of various types of self-propelling particles, ranging in size from nanometers to millimeters.[22,23]

In active matter systems, the activity of constituent particles leads to the emergence of active stresses, which act in addition to the usual equilibrium ones such as nematic or viscous stresses.[4,17,24] For example, in a bacterial colony of *E. coli*, the dynamics are driven by viscous, elastic, and active stresses, with bacterial hydrodynamic propulsion creating extensional flow fields that pull in fluid from the sides and push it out along the bacterial axis.[25,26] In the absence of activity, the dynamics reduce to nematohydrodynamic behavior of nematic liquid crystals.[27] Following this pathway, it is tempting to define the trace of the total nonequilibrium stress tensor as an effective active pressure.

The physical meaning of such an effective active pressure intuitively can be understood as the pressure on the boundary to confine active particles in space,[28,29] analogous to the kinetic theory of gases, where collisions between molecules and container walls generate pressure, or similar to the Brownian osmotic pressure generated by molecules or colloidal solutes in a solution. However, a key feature of active matter is that it is inherently in a thermodynamic nonequilibrium state, making its collective behavior impossible to understand using conventional statistical mechanics.[30,31] In equilibrium systems, pressure is a state function that appears consistently in the equations of state for gases, liquids, and even solids. Examples include the ideal gas law, the Van der Waals equation and the Carnahan–Starling and Hall equations for hard spheres.[32–34] Pressure attains the same value whether derived

†Corresponding author. E-mail: joscha.mecke@szu.edu.cn

‡Corresponding author. E-mail: yongxiang.gao@szu.edu.cn

© 2025 Chinese Physical Society and IOP Publishing Ltd. All rights, including for text and data mining, AI training, and similar technologies, are reserved.

from microscopic momentum flux, statistical thermodynamics or hydrodynamics. While some of these definitions are extended to define pressure in active matter systems, their convergence and the existence of an equation of state are by no means guaranteed,[28,35–37] which renders the understanding and physical interpretation of pressure in active matter a challenging problem.

The conceptual understanding of active stresses and effective pressure is still in early stages, with different perspectives developed. Considerable discussion has centered on the conditions under which active pressure can be regarded as a state function — governed by internal momentum flux — and on the circumstances in which this description breaks down, causing the mechanical pressure on the confining wall to deviate from that derived from the bulk.[35,38–40] Despite these challenges, active pressure remains a valuable concept for understanding collective behaviors such as self-assembly, phase separation, or pattern formation in active matter systems,[13,14,17,41–43] controlling self-propelled particles,[39] as well as for designing and fabricating micromachines.[44,45]

In this paper, we conduct a synthesis review on past studies of active pressure, exploring the microscopic mechanical origins especially in active Brownian particles. We start from the simple ABP model, demonstrating that in this system the active pressure behaves as a state function and exhibits a nontrivial dependence on density. As part of the broader effort to extend equilibrium concepts to nonequilibrium situations and thereby apply well-known results to complex systems, researchers have sought to explain the active pressure of the simple ABP model by drawing analogies to pressure in equilibrium systems, introducing the concepts of effective temperature and effective adhesion. Going beyond the simplest ABP models has revealed that pressure-based equations of state are highly sensitive and can fail when influenced by factors such as density-dependent propulsion speeds, torques, and complex boundary shapes or interactions. Here we trace these developments, highlight the key mechanisms behind the breakdown of the equation of state, and discuss how these insights inform both theoretical modeling and experimental design in active matter research.

2. Pressure in equilibrium systems

2.1. Pressure in an ideal gas

In the ideal gas, the simplest and most widely used model in statistical mechanics, the pressure can be shown to arise from the collective impact of gas particles colliding with the walls of the container (Fig. 1(a)). These collisions transfer momentum to the walls, and the frequency and strength of these collisions are directly related to the thermal energy of the particles, $k_{\mathrm{B}}T$, where k_{B} is the Boltzmann constant and T is the absolute temperature. This leads to the well-known expression for the ideal gas pressure[46]

$$P_{\mathrm{id}} = nk_{\mathrm{B}}T, \tag{1}$$

where $n = N/V$ is the number density, with N the total number of gas molecules and V the volume of the container.

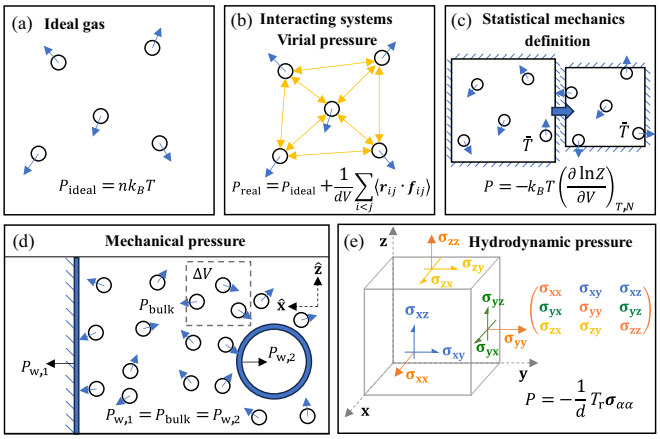


Fig. 1. Different definitions of pressure in equilibrium systems. (a) Pressure in an ideal gas. (b) Virial pressure contributed by intermolecular interactions. (c) Pressure defined based on statistical mechanics. (d) Mechanical pressure defined as the force per unit area on the confining boundaries or walls; $P_{\mathrm{w},1}$ and $P_{\mathrm{w},2}$ represent the mechanical pressure on a flat wall and a curved wall, respectively. The pressure is uniform throughout the system, such that $P_{\mathrm{w},1} = P_{\mathrm{w},2} = P_{\mathrm{bulk}}$. (e) Pressure is also defined as the sum of the trace of the hydrodynamic stress tensor.

2.2. Virial pressure due to interactions between particles

For realistic systems, interactions between particles also contribute to the pressure in the system (Fig. 1(b)), which can be calculated via the virial theorem.[47] It provides a foundational route to define pressure in many-body systems from a microscopic perspective, relating the average force acting between particles to the macroscopic pressure via the spatial distribution of particles and their mutual interactions. For a system of N particles confined in a volume V in d dimensions, the pressure can be written as

$$P_{\mathrm{V}} = \frac{1}{\mathrm{d}V}\sum\nolimits_{i<j}\langle \boldsymbol{r}_{ij}\cdot\boldsymbol{f}_{ij}\rangle, \tag{2}$$

where $\boldsymbol{f}_{ij}$ and $\boldsymbol{r}_{ij}$ denote the force and relative distance between two particles i and j, respectively. Here, the dot product quantifies how pairwise forces contribute to the net momentum exchange and hence to the pressure. This formulation offers an intuitive way to compute pressure in molecular simulations. The concept can also be applied to suspensions of Brownian particles where entropy drives the colloids to spread out leading to an osmotic pressure analogous to the reasoning above.[48]

2.3. Statistical definition

In statistical mechanics, macroscopic thermodynamic quantities can be derived from the microscopic properties of

the system through the partition function Z, which encodes the statistical weight of all possible microstates.[49] Take canonical ensemble as an example. The partition function is defined as

$$Z = \int \mathrm{e}^{-H(p,q)/k_\mathrm{B}T}\,\mathrm{d}p\mathrm{d}q, \tag{3}$$

where $H(p,q)$ is the Hamiltonian of the system, p and q represent momentum and coordinate, respectively. In this case, pressure can be expressed as a derivative of the partition function with respect to volume

$$P = -k_\mathrm{B}T\left(\frac{\partial \ln Z}{\partial V}\right)_{T,N}. \tag{4}$$

This expression conveys the fundamental thermodynamic definition of pressure, relating it to changes in the system's accessible microstates and entropy with volume (Fig. 1(c)), i.e., pressure is understood to originate from the volume dependence of the partition function, rather than from a purely mechanical or kinetic description.

2.4. Mechanical definition

Generally, pressure is understood as the normal force exerted per unit area on a surface or a wall (Fig. 1(d))[50]

$$P = \frac{F}{A}, \tag{5}$$

where F is the total normal force and A is the total surface area over which the force is applied.

By explicitly expressing the particle–wall interaction potential $\Phi(x)$, and taking its derivative with respect to the particle–wall separation x , one obtains the term corresponding to the force exerted on the wall.[35] Thus, the mechanical pressure can be defined and computed via

$$P = \int_0^\infty n\,(x)\,\partial_x \Phi\,(x)\,\mathrm{d}x. \tag{6}$$

This mechanical definition can be proved to be equivalent to the thermodynamic pressure on the wall for equilibrium systems.[35] This equation still holds even if the system contains other types of particles (such as solvent molecules), as long as those particles do not exert any direct force on the wall (i.e., the wall is semipermeable to them),[35] in which case the pressure P is identified as the osmotic pressure. Note that this mechanical definition remains valid regardless of whether the system is in equilibrium or not.

2.5. Hydrodynamic definition

In hydrodynamics, pressure arises as a macroscopic, continuum field that captures the isotropic part of the stress tensor in a fluid.[50] The pressure is defined as the sum of the trace of stress tensor $\boldsymbol{\sigma}$ divided by the dimension d,[51]

$$P = -\frac{1}{d}\sum_{\alpha=1}^{d}\boldsymbol{\sigma}_{\alpha\alpha}. \tag{7}$$

Note that it is fundamentally different from the microscopic virial expression, but connected through coarse-graining.

3. Pressure in active systems

As active matters consume energy from the environment, they are inherently driven out of equilibrium.[17] The question then is how to define pressure in active systems. To make progress, ABP models have been used in simulations and theoretical calculations due to their simplicity. It is generally accepted that pressure in active systems contains two contributions[28,35–37,52–55]

$$P = P_\mathrm{p} + P_\mathrm{swim}. \tag{8}$$

One is the common pressure experienced in a passive system, denoted as P_p, and the other is contributed by the self-propelled motion of particles, known as swim pressure,[28] P_swim. The passive part of the pressure can be further expressed as the sum of two terms

$$P_\mathrm{p} = P_\mathrm{id} + P_\mathrm{V}, \tag{9}$$

where P_id and P_V denote the ideal-gas like contribution from random Brownian motion of particles and the virial contribution arising from mutual interactions.

In the past decade, various approaches to derive expressions for pressure in active matter have been explored.[28,35,37,42,52,53,56,57] Though pressure is a state function in equilibrium systems, it is far from clear what to expect in active matter due to its far-from-equilibrium nature. It becomes even more complicated in the presence of various confining boundaries,[52] which may alter the spatial distribution and dynamics of particles. Indeed, it has prompted extensive discussion whether, and under what conditions, pressure qualifies as a state function, thereby providing an opportunity to further develop the statistical physics of nonequilibrium systems.

3.1. Active Brownian particles

Active Brownian particles are a class of models composed of particles that possess self-propulsion.[58] The propulsion speed and direction are influenced by noise, friction, and

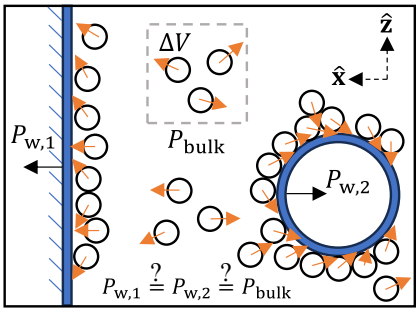


Fig. 2. Pressure in ABP model systems. $P_{\mathrm{w},1}$ and $P_{\mathrm{w},2}$ are mechanical pressures at flat and curved walls, respectively. P_{bulk} represents bulk pressure away from boundaries in active system.

external fields. The particle's orientation evolves over time, which can be driven by rotational Brownian motion, deterministic torques, or a combination of both. ABPs model "dry" active systems without hydrodynamic coupling. Our discussion mainly revolves around this model to explore the conditions under which an equation of state holds and the situations where it breaks down (Fig. 2).

3.2. Irving–Kirkwood formalism for stress tensor

The microscopic definition of the stress tensor in statistical mechanics is commonly formulated using the Irving–Kirkwood (IK) formalism, first developed in 1950. In this framework, the stress tensor is defined as the flux of linear momentum across a surface element, derived from the conservation laws applied at the microscopic scale. It contains contributions from both kinetics and configurations, representing the momentum transport due to particle motion and interparticle interactions, respectively. The IK stress tensor for a system of N particles interacting via pairwise forces can be expressed as

$$\begin{aligned}\boldsymbol{\sigma}(\boldsymbol{r},t) = & -\sum_i m_i v_i v_i \delta(\boldsymbol{r}-\boldsymbol{r}_i) \\ & -\frac{1}{2}\sum_{i\neq j}\boldsymbol{r}_{ij}\boldsymbol{F}_{ij}\int_0^1 \delta(\boldsymbol{r}-\boldsymbol{r}_i+\lambda\boldsymbol{r}_{ij})\mathrm{d}\lambda. \quad (10)\end{aligned}$$

Here, $\boldsymbol{r}_{ij}=\boldsymbol{r}_i-\boldsymbol{r}_j$, m_i is the mass of particle i, and $\boldsymbol{F}_{ij}$ is the force exerted on particle i by particle j. The first term represents the momentum carried by the particles. The second term accounts for the contribution from interparticle forces, integrated along the line connecting particles i and j, with the force contribution distributed uniformly over the entire segment.

3.3. Swim pressure as the trace of swim stress tensor

The IK formalism provides a well-established framework for defining the stress tensor in particle-based systems. To describe stress in active matter, the IK formalism has been further extended to incorporate nonequilibrium contributions from active forces.

To put into account the contribution from persistent propulsion of active particles, swim stress for overdamped systems is defined in the spirit of the IK formalism,[28,37]

$$\boldsymbol{\sigma}_{\mathrm{swim}} = -n\langle \boldsymbol{r}\boldsymbol{F}_{\mathrm{swim}}\rangle. \quad (11)$$

In this case, the force is replaced by the effective self-propulsion force $\boldsymbol{F}_{\mathrm{swim}}$.

While the swim stress provides a tensorial description of momentum flux, the pressure can be obtained by taking its trace.[59] That is, swim pressure corresponds to the sum of the diagonal components of the swim stress tensor,

$$P_{\mathrm{swim}} = -\frac{1}{d}\sum_{\alpha=1}^{d}\boldsymbol{\sigma}^{\mathrm{swim}}_{\alpha\alpha}. \quad (12)$$

This scalar definition of swim pressure as the trace of the swim stress tensor can also be understood from a complementary perspective: an extension of the virial theorem.[47] Swim pressure has been recast in a virial-like form involving the dot product of the self-propulsion force and particle position,[53,60,61]

$$P_{\mathrm{swim}} = \frac{1}{dV}\sum_i^N \langle \boldsymbol{F}_i^{\mathrm{swim}}\cdot\boldsymbol{r}_i\rangle. \quad (13)$$

Here, conservative pairwise forces are replaced by swim forces, so that the virial theorem remains a useful framework for interpreting active pressures in nonequilibrium systems.[28]

4. Pressure is a state function in specific ABP models

4.1. Overdamped simple ABP model

To understand the emergence of active stresses and pressure in nonequilibrium systems, researchers have focused on simple overdamped active Brownian particle (simple ABP) systems. In this model, active particles evolve via a Langevin equation of motion

$$\zeta\dot{\boldsymbol{r}}_i(t) = \zeta U_0\boldsymbol{n}_i(t) + \boldsymbol{F}_i + \boldsymbol{\xi}_i(t), \quad (14)$$

where $\boldsymbol{r}_i(t)$ is the particle location, U_0 is the constant swimming speed, $\boldsymbol{n}_i(t)$ is the unit vector along the axis of self-propulsion, ζ is the friction from the suspending fluid, $\boldsymbol{\xi}_i(t)$ is the thermal random force, and $\boldsymbol{F}_i$ includes forces on the particle from pairwise interactions and external fields. The random force satisfies $\langle\boldsymbol{\xi}_i(t)\rangle = 0$ and $\langle\boldsymbol{\xi}_i(t)\cdot\boldsymbol{\xi}_i(0)\rangle = 2dk_{\mathrm{B}}T\zeta\delta(t)$.

4.1.1. Pressure in overdamped simple ABP models

In ABP models, the active swim force on a particle is

$$\boldsymbol{F}_{\mathrm{swim}} = \zeta U_0\boldsymbol{n}(t). \quad (15)$$

By substituting Eq. (15) into Eq. (13), the swim pressure becomes

$$P_{\mathrm{swim}} = \frac{\zeta U_0}{dV}\sum_i^N\langle\boldsymbol{n}_i\cdot\boldsymbol{r}_i\rangle. \quad (16)$$

It has further been shown that P_{swim} can be expressed as[52]

$$P_{\mathrm{swim}} = \frac{n}{dD_{\mathrm{R}}}\zeta U_0 U_\phi, \quad (17)$$

where U_ϕ represents the average particle velocity projected along its swimming direction at various packing fraction ϕ,

$$U_\phi = \frac{1}{N}\sum_i^N\langle\boldsymbol{n}_i\cdot\dot{\boldsymbol{r}}_i\rangle. \quad (18)$$

Here, one velocity factor U_0 is preserved while the other is replaced by a density-dependent speed U_ϕ. Here $\phi = nv_{\mathrm{p}}$,

the volume fraction in $3d$, and $\phi = n\sigma_{\rm p}$, the area fraction in 2d, where $v_{\rm p}$ and $\sigma_{\rm p}$ are the volume and area of a particle, respectively. Physically, U_ϕ measures how much of the self-propulsion is preserved in the actual motion of the particles after accounting for collisions and interactions, which serves as a key kinetic parameter for swim pressure.[52,53,57,60]

In the dilute regime, $U_\phi = U_0$. The swim pressure given in Eq. (17) is then reduced to

$$P^0_{\rm swim} = \frac{\zeta n U_0^2}{dD_{\rm R}}, \tag{19}$$

which has been reported in multiple studies[28,37,53] for both two- and three-dimensional systems. In both cases, the pressure introduced by activity is proportional to U_0^2 (Fig. 3), revealing the fundamental origin of active pressure.

In dense simple ABP systems, the swim pressure is decreased because the orientation of the active particles changes on the timescale $\tau_{\rm R}$ such that the particles do not necessarily reorient when colliding and thus mutually obstruct the active dynamics.[28,37,52,53,57,60,62] That is, U_ϕ is no longer equal to U_0, but instead decreases with packing fraction,[37]

$$U_\phi = U_0\,(1-\lambda\phi)\,. \tag{20}$$

Here λ is a constant parameter, characterizing the slope of the decrease in average particle propulsion speed with packing fraction ϕ.

By using active microrheology, the leading-order correction to the swim pressure is found to be a linear decrease with density[28] (Fig. 3(a))

$$\frac{P_{\rm swim}}{P^0_{\rm swim}} = 1-\phi. \tag{21}$$

On the other hand, interparticle forces (steric repulsion) have a positive contribution to the overall pressure, which increases linearly with the particle density in the leading order. Thus, the full pressure is obtained as

$$\frac{P}{P^0_{\rm swim}} = 1-\phi\,(1-3Pe_{\rm R}) + \mathcal{O}\left(\phi^2\right), \tag{22}$$

where $Pe_{\rm R} = U_0/(aD_{\rm R})$ is the rotational Peclét number, and a is the particle radius.

This equation can be understood as an expansion of the equation of state of active matter in terms of deviations from the effective ideal gas state. The negative term (the second term of the right-hand side of the equation) plays a similar role to the second-virial coefficient of equilibrium colloidal systems, and when it is negative, it indicates effective attractive interactions between the active particles.[63]

In Gompper's study,[53] the pressure collapses onto a common curve described by

$$\frac{P}{P^0_{\rm swim}} = 1-\kappa\phi, \tag{23}$$

with κ of order unity. This form can be derived by combining Eqs. (17) and (20), which captures the ideal-gas-like pressure at low ϕ and the suppression at higher densities, reflecting the onset of interaction effects in active systems.

The above corrections to the swim pressure/pressure can well capture the results obtained in various simulations of simple ABPs in the dense regime, as shown in Fig. 3.

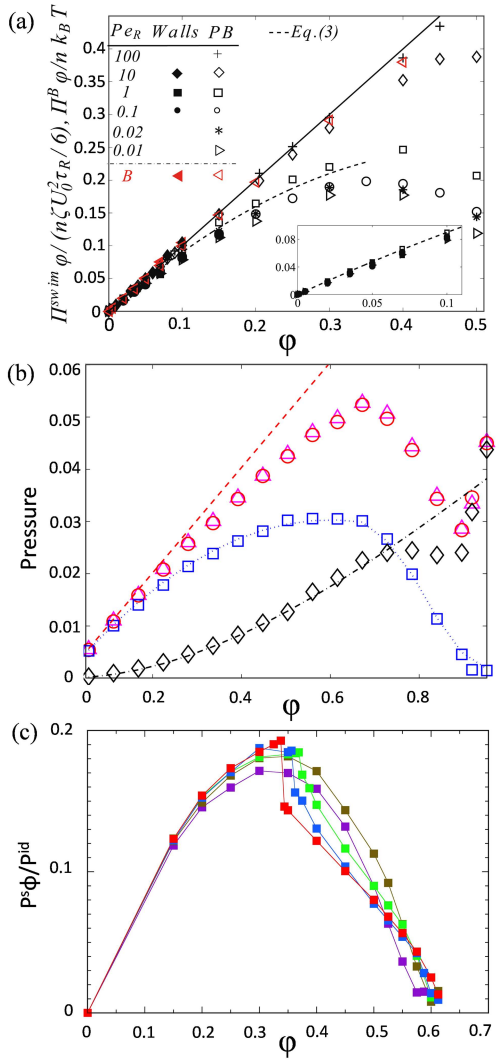


Fig. 3. The dependence of simple ABPs' pressure on packing fraction. (a) The swim pressure and Brownian pressure at different $Pe_{\rm R}$ with periodic boundary conditions (PB) and walls. The solid black line corresponds to a linear increase of pressure with packing fraction. The dashed curve is the dilute theory expression. Reused with permission from Ref. [28]. Copyright (2014) by the American Physical Society. (b) Total pressure calculated from the IK formula (magenta triangles) and with the force on the walls (magenta circles). Pressure following an active ideal gas law (magenta dashed line), passive pressure from pairwise interactions (measured in simulation, black diamonds; theory, black dash-dot line) and the swim pressure (simulation, blue squares; theory, blue dot line) are also presented. Reused with permission from Ref. [37]. Copyright (2014) by the Royal Society of Chemistry. (c) Swim pressure at various $Pe_{\rm R}$ (9.8, purple; 29.5, olive; 44.3, green; 59.0, blue; and 295.0, red). Reproduced from Ref. [53]. ©The Royal Society of Chemistry, CC BY 3.0.

4.1.2. Effective temperature in the dilute regime

The relationship between swim pressure and density in dilute situation has been explored in active colloidal suspensions through sedimentation experiments.[56] To further char-

acterize the thermodynamic properties of such self-propelled systems, a method based on the equilibrium fluctuation–dissipation theorem has been proposed for defining an effective temperature.[64] Félix Ginot and his colleagues designed the experimental setup shown in the inset of Fig. 4(a). They tilted the system by a small angle θ along the z direction to form a continuous two-dimensional monolayer of gold-platinum Janus microspheres immersed in a hydrogen peroxide bath at the bottom of the observation chamber, establishing varying packing fractions along the z axis by balancing the osmotic pressure with the gravitational potential. The simulation results also agree well with the experimental results (Fig. 4(b)). In the long-time limit of the ABP dynamics, the particles can be regarded as diffusing with an activity-induced effective diffusion coefficient,[65,66] $D_{\rm eff} = U_0^2 \tau_{\rm R}/d$.

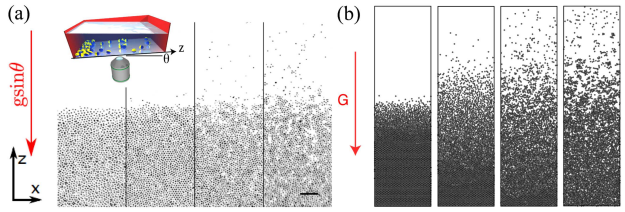


Fig. 4. Sedimentation equilibrium of self-propelled particles in experiments and simulations. (a) Sedimentation profiles of phoretic gold–platinum Janus colloids; activities increase from left to right. (b) Simulation snapshots for self-propelled hard disks under gravity; activities increase from left to right. Reproduced from Ref. [56], ©Félix Ginot, published by APS, CC BY 3.0.

In dilute situations, the steady-state distribution in the gravitational potential follows a Boltzmann distribution thermalized at $T_{\rm eff}$,

$$\mathcal{P}(z) \propto \exp\left[-\frac{mgz\sin\theta}{k_{\rm B}T_{\rm eff}}\right], \tag{24}$$

which defines an effective temperature.

Moreover, it has also been shown experimentally that in dilute suspensions an effective Stokes–Einstein relation can be established,[56] i.e., $k_{\rm B}T_{\rm eff}/\zeta = D_{\rm eff}$, which implies $k_{\rm B}T_{\rm eff} = U_0^2\tau_{\rm R}\zeta/d$. The swim pressure of dilute simple ABPs, as shown in Eq. (19), thus can be expressed in the form of an ideal gas law, with temperature replaced by an effective temperature:

$$P_{\rm swim} = nk_{\rm B}T_{\rm eff}. \tag{25}$$

A similar conclusion has been obtained by Solon *et al.* in a simulated system.[35]

The relation between the effective temperature $T_{\rm eff}$ and the self-propulsion can be easily derived,[56,67] which can be expressed as a function of the translational Péclet number ($Pe_{\rm s} = aU_0/D_0$),

$$\frac{T_{\rm eff}}{T} = \left(1+\frac{2}{9}Pe_{\rm s}^2\right). \tag{26}$$

This theoretical prediction can well capture the experimental results obtained in self-propelled Janus colloids, as shown in Fig. 5.

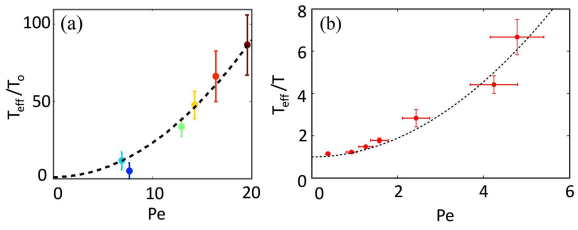


Fig. 5. Effective temperature $T_{\rm eff}$ as a function of translational Péclet number $Pe_{\rm s}$ measured in experimental systems. (a) Self-propelled Pt/Au Janus colloids in H_2O_2 solution. Reproduced from Ref. [56], ©Félix Ginot, published by APS, CC BY 3.0. (b) Self-driven Pt/PS Janus colloids in H_2O_2 solution. Reused with permission from Ref. [67], Copyright (2010) by the American Physical Society. In both studies, experimental results (symbols) are directly compared with theoretical predictions (dashed line), which exhibit a quadratic scaling relation. Both studies demonstrate quantitative agreement with theoretical predictions across a broad range of activity strengths.

Overall, experimental and simulation studies collectively indicate that, in the dilute limit, systems composed of simple ABPs exhibit behaviors analogous to those of an ideal gas. In particular, these studies show that such active systems can be effectively described using the concept of an activity-dependent effective temperature $T_{\rm eff}$, which captures how self-propulsion modifies their thermodynamic and mechanical properties compared to equilibrium systems. Under dilute and weak activity conditions, this analogy allows researchers to employ familiar equilibrium statistical mechanical tools. However, beyond this regime, significant deviations are expected, as shown by Baek *et al.*,[68] where the absence of a Boltzmann distribution defies the application of such equilibrium concepts.

It is worth noting that if the Brownian motion of the particles stemming from the thermal agitation of the active colloids is much stronger than the active contributions, the contributions of the effective active pressure will be hidden in the thermal equilibrium dynamics of the colloids.[28] The importance of the thermal contributions is typically measured with the translational Peclét number $Pe_{\rm s}$. Measurements are more precise for $Pe_{\rm s}$ above 10, since the thermal agitation cannot be turned off in experiments, this is a crucial factor for experimental design.

4.1.3. Effective adhesion at finite densities

The existence of swim pressure has been explicitly confirmed in a suspension of self-propelled Janus colloids subject to an acoustic confinement of size much larger than the colloids themselves.[69] These self-propelled particles swim via self-diffusiophoresis[70] in a hydrogen peroxide solution. Adding a harmonic force $k(\boldsymbol{r}(t) - \boldsymbol{r}_0)$ leads to a balance between the active and the confinement forces, where k is the spring constant of acoustic confinement, $\boldsymbol{r}(t)$ is the particle

position at time t. Upon sudden release, the system exhibited a "crystal explosion" (Fig. 6(a)), reflecting the tendency of active particles to escape in the absence of confinement. This observation directly illustrates the physical origin of the swim pressure, which is the mechanical pressure exerted by active particles as a result of their self-propulsion.[28,29] Furthermore, the pressure decreases with increasing trap stiffness k (Fig. 6(b)). The strong trap reduces the "moment arm", defined as the path length that active particles travel before reorienting. Such confinement thus results in a decreased swim pressure. At finite densities, particle obstructions and collisional slow-down effects effectively shorten the moment arm, leading to a further decrease in the swim pressure as the density increases.

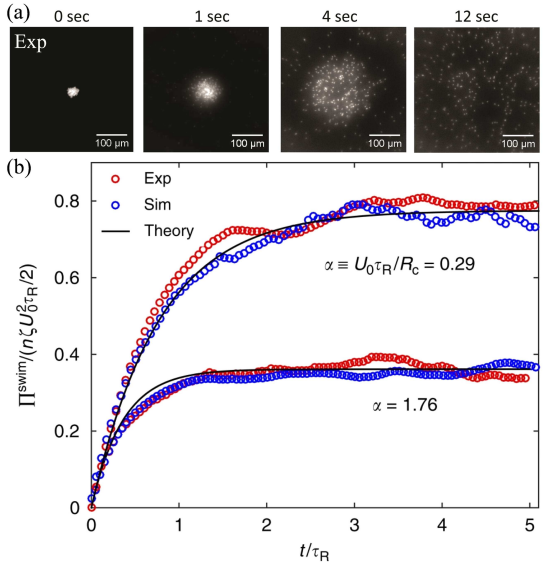


Fig. 6. Crystal explosion experiment. (a) Experimental observation of an active crystal rapidly expanding after acoustic trap released, showing a transition from a dense cluster to a diffusive steady state. (b) Swim pressure of Janus particles under different confinement strengths ($\alpha = U_0\tau_R/R_C$), where $R_C = \zeta U_0/k$ is the trap size. Red and blue dots show experimental and simulation results, and black lines are theoretical predictions. Reproduced from Ref. [69] under CC BY 4.0.

At high particle density, an effective attractive interaction or adhesion emerges between active particles, from which an effective adhesion strength could be extracted. Based on this, a unique scaling law relating activity to self-propulsion was identified in both sedimentation experiments and simulations.[56] At finite densities, both experimental and numerical results show that the functional form of the equation of state changes continuously with increasing activity. This change cannot be fully explained by introducing an effective temperature as in Subsection 3.1.2, highlighting the limitations of this approach in describing active systems.

The behavior of the active system was effectively mapped onto the Baxter model,[71] which describes an equilibrium fluid with adhesive interactions. In this model, particle interactions are described by a square-well potential consisting of a hard-core repulsion at short distances and a narrow attractive well just beyond the particle diameter. The attractive interaction is short-ranged, and its strength is quantified by a dimensionless adhesion parameter A. The pressure–density relation can then be expanded as

$$Z = \frac{P}{nk_BT} = 1 + b_1\phi + b_2\phi^2 + \mathcal{O}\left(\phi^3\right). \tag{27}$$

The first two virial coefficients are known analytically,[72] with $b_1 = 2 - A$, $b_2 = \frac{25}{8} - \frac{25}{8}A + \frac{4}{3}A^2 - 0.122A^3$. That is, when A increases, the pressure changes from the monotonic hard-particle behavior to a nonmonotonic density dependence for $A > 2$ as the initial slope given by b_1 then becomes negative. The effective adhesion A increases with self-propulsion as a function of effective temperature (Fig. 7)

$$A \sim \sqrt{T}_{\text{eff}}/T. \tag{28}$$

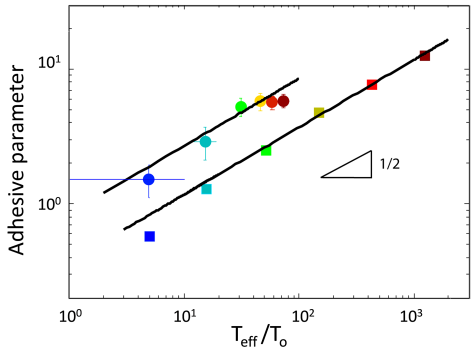


Fig. 7. Adhesive parameter A as a function of T_{eff}/T_0. Scaling relation of $A \sim \sqrt{T_{\text{eff}}/T_0}$ was revealed in both experiments (circles) and simulations (squares). Solid lines indicate the expected slope of $1/2$ with different prefactors. Reproduced from Ref. [56]. ©2015 American Physical Society, CC BY 3.0.

The pressure in active systems remains describable by an equation of state even after introducing the effective adhesion parameter A. This indicates that the incorporation of effective adhesive interactions among active particles does not compromise the thermodynamic consistency of the system. Instead, it expands the applicability of the equation of state, enabling it to account for more complex phenomena such as clustering and motility-induced phase separation.

4.1.4. Motility induced phase separation

In ABP systems, phase separation into dilute and dense regions can occur even in the absence of apparent attractive interactions.[5,73–75] For example, motility induced phase separation (MIPS) arises from accumulation of self-propelled particles in regions where they move more slowly.[76] The slow down may happen through direct collisions[74,75,77] or density-dependent propulsion speed such as quorum sensing.[78–82]

In the ABP system, the coexistence of dilute and dense phases depends on the Peclét number and particle densities.[74,75,83] For low Pe_R and finite ϕ, a bimodal distribution of the packing fraction is obtained, indicating phase coexistence of an active gas and a cluster phase.[5,77,84]

Such phase coexistence behavior can be explained to a large extent by making an analogy to passive particles with attractive interactions. The Baxter model for adhesive particles can be used to understand the phase behavior in ABP systems observed in simulations and experiments by using effective adhesion.[56] Moreover, the non-monotonic behavior in Eq. (22) has been reproduced in simulations, where the total pressure at $\phi = 0.6$ is lower than that at $\phi = 0.3$ for a value of $Pe_{\mathrm{R}} \approx 0.03$, i.e., when the second term on the right-hand side of Eq. (22) is negative.[28]

Systematic studies[5,60,83,85] on the pressure behavior of spherical ABPs undergoing MIPS — particularly regarding the applicability of an equation of state to such nonequilibrium transitions — have revealed that the liquid-gas phase coexistence and transition in ABP systems resemble equilibrium first-order phase transitions, characterized by a flat pressure plateau between the coexisting phases. It suggests that pressure equalization occurs once nucleation has taken place. When nucleation is suppressed (e.g., in open systems without walls), the system remains in a metastable homogeneous state.[60] In this case, no Maxwell construction applies, and the large structural differences between the coexisting phases lead to a high nucleation barrier.[60,83] Nevertheless, the effective active pressure can be determined by bulk correlators, showing that the pressure is not determined by the interactions with the walls, similar to that in equilibrium systems. Additionally, the interfacial tension between the two phases is very large (compared to equilibrium systems) and negative, which would imply an energy reward if the interface is increased.[85] These findings underscore the fundamental differences between MIPS in active systems and phase separation in equilibrium fluids, especially in the role of interfacial contributions and the breakdown of classical thermodynamic constructs such as the Maxwell construction. They emphasize the need for further theoretical and experimental studies to clarify how boundary conditions, interfacial properties, and nucleation dynamics jointly shape the phase behavior of active matter.

4.2. Underdamped simple ABP model

To extend the applicability of active pressure theories to mesoscopic and macroscopic regimes, it is necessary to account for inertial effects in active particle models. The underdamped simple ABP model introduces finite mass m into the description of torque-free, spherical, self-propelled particles, thereby in the general case retaining both translational and rotational inertia in the particle dynamics.

The translational and rotational motion is governed by the Langevin equation with inertia

$$m\ddot{\boldsymbol{r}}_i(t) = -\zeta\dot{\boldsymbol{r}}_i(t) + \zeta U_0\boldsymbol{n}_i(t) + \boldsymbol{F}_i + \boldsymbol{\xi}_i(t). \tag{29}$$

$$I\ddot{\theta}_i(t) = -\zeta_{\mathrm{R}}\dot{\theta}_i(t) + \xi_{\mathrm{R},i}(t), \tag{30}$$

where I is the moment of inertia of a particle, $\xi_{\mathrm{R},i}$ is white noise associated with rotation. This underdamped case allows for the analysis of stress generation under finite inertia. Compared to the overdamped case, the underdamped model captures key physical phenomena such as delayed reorientation, finite response times, and the emergence of Reynolds stress, all of which significantly affect the definition and measurement of active pressure.

4.2.1. Swim–Reynolds pressure compensation in dilute regime

In the case of confining harmonic walls, application of the virial theorem shows that the swim pressure can be expressed as[86]

$$P_{\mathrm{swim}} = \frac{N}{L^2}\frac{m^2U_0^2}{St}\left(\frac{1}{1+\omega_0^2\tau^2}\right), \tag{31}$$

where ω_0 is the characteristic frequency of oscillation, $St = (m/\zeta)/\tau$ is the translational Stokes number, and τ is the persistence time. Specifically, when $\omega_0\tau < 1$, the swim pressure initially increases with τ. However, when the persistence time τ exceeds a critical value (i.e., $\tau > 1/\omega_0$), the swim pressure starts to decrease. From the equation, it can be seen that when St is large, the inertial effects of the particle become significant such that they cannot quickly respond to the propulsion force, leading to a lag in its direction.[87] It is discussed in Ref. [87] that the inertial lag between particle orientation and direction of movement reduces the correlation $\langle \boldsymbol{r}\boldsymbol{F}_{\mathrm{swim}}\rangle$ between the "momentum arm" $\boldsymbol{r}$ and the swim force $\zeta U_0\boldsymbol{n}(t)$, which explicitly depends on the particle orientation. This effect is captured by the rotational Stokes number $St_{\mathrm{R}} = (m/\zeta)/\tau_{\mathrm{R}}$, which measures the ratio between inertial relaxation time and rotational diffusion time. The swim stress diminishes as

$$P_{\mathrm{swim}} = nk_{\mathrm{s}}T_{\mathrm{s}}\frac{1}{1+2St_{\mathrm{R}}}, \tag{32}$$

where $k_{\mathrm{s}}T_{\mathrm{s}}$ denotes swim "energy scale", defined in three dimensions as $kT_{\mathrm{s}} \equiv \zeta U_0^2\tau_{\mathrm{R}}/6$. Although the swim pressure is reduced by the inertia effects, inertia introduces an additional kinetic stress (Reynolds stress) term, consisting of the Brownian osmotic stress and a contribution stemming from self-propulsion which depends on St_{R}.

$$P_{\mathrm{Rey}} = nk_{\mathrm{B}}T + nk_{\mathrm{s}}T_{\mathrm{s}}\frac{2St_{\mathrm{R}}}{1+2St_{\mathrm{R}}}. \tag{33}$$

Interestingly, the decrease in swim stress is exactly compensated by the increase in kinetic stress (Reynolds stress)

$$P_{\mathrm{swim}} + P_{\mathrm{Rey}} = n(k_{\mathrm{B}}T + k_{\mathrm{s}}T_{\mathrm{s}}), \tag{34}$$

so that the total pressure remains invariant with respect to inertia in dilute systems. This compensation indicates that the equation of state still holds for underdamped ABPs in the

dilute regime, despite the redistribution of momentum flux among different stress contributions.

Furthermore, a conceptual revision of the swim stress formulation has revealed deeper insights into the distinction between local and global pressure definitions in underdamped models.[88] Early studies on overdamped ABPs concluded that the bulk pressure of ideal active particles is equivalent to that of passive gases, as the swim stress was thought to vanish in the bulk,[57] which led to the belief that active pressure arises solely from particle–wall interactions. However, this conclusion does not hold in general condition, such as in the presence of interia. The conventional formulation of swim stress vanishes locally and thus fails to capture internal momentum transfer. In contrast, the inertial-based formulation gives a finite local swim stress, which aligns with previous discussions in Ref. [89].

4.2.2. Modified EOS at finite concentration

At finite concentrations, the total pressure of active systems can still be described by a modified mechanical pressure theory, provided that both the Reynolds stress and interparticle interaction pressure are explicitly included.[87,89] In the high-density regime, active particles exhibit pronounced phase separation and self-assembly behaviors, and their mechanical response becomes increasingly complex. Simulations reveal that both the swim pressure and Reynolds pressure decrease with increasing particle volume fraction ϕ, primarily due to frequent collisions that limit self-propulsion and reduce the correlation in particle motion. Specifically, the swim pressure exhibits a concentration dependence

$$P_{\text{swim}} = nk_{\text{s}}T_{\text{s}}\frac{1-\phi-\phi^2}{1+2St_{\text{R}}}. \tag{35}$$

Meanwhile, the Reynolds pressure follows a similar form

$$P_{\text{Rey}} = nk_{\text{s}}T_{\text{s}}\frac{1-\phi-\phi^2}{1+1/(2St_{\text{R}})} + nk_{\text{B}}T. \tag{36}$$

The sum is obtained as

$$P_{\text{swim}} + P_{\text{Rey}} = nk_{\text{B}}T + nk_{\text{s}}T_{\text{s}}\left(1-\phi-\phi^2\right). \tag{37}$$

Notably, the sum of swim and Reynolds pressures, i.e., the total active pressure, remains independent of the Stokes number St_{R} at fixed Péclet number, but exhibits a strong dependence on concentration ϕ. In addition, repulsive interactions between particles introduce a non-negligible interparticle (collisional) pressure, which increases monotonically with ϕ and contributes to the stabilization of the system.

Therefore, these results highlight the crucial role of inertia in capturing the true contribution of active forces to the system's internal stress, and further demonstrate that the pressure in underdamped simple ABPs obeys an equation of state.

5. Pressure is not a state function in generic active systems

The validity of an equation of state in underdamped active matter systems is highly sensitive to system details. In dilute spherical active Brownian particle systems without torque, previous studies have shown that pressure remains a state function even when particle inertia is finite.[87,89] While the equation of state may hold for simple, dilute, and torque-free ABPs, it does not apply to more complex active systems.[35,40,90,91]

5.1. Torque between particles

Interparticle alignment torque is one of the most extensively studied interactions in active matter.[17] A key mechanism breaking the equation of state in active matter is to introduce torque between particles via non-central, anisotropic interactions.[35]

The orientation of each ABP evolves under an aligning torque generated by neighboring particles, with strength set by the rotational mobility.[35] This torque depends explicitly on the relative positions and orientations of particles, making the interaction anisotropic and non-central. As a result, the particle distribution becomes sensitive to the wall potential, and the mechanical pressure depends not only on bulk variables but also on the microscopic details of the alignment rule and boundary geometry.

For example, in the visual perception model of Bechinger *et al.*,[92] particles sense neighbors within a finite visual cone and adjust propulsion speed according to the perceived density. This anisotropic sensing induces an effective alignment torque, which becomes non-reciprocal for asymmetric cones ($\alpha < \pi$). As a result, mechanical pressure depends on the specific interaction rule and boundary geometry, rather than solely on bulk variables. Simulations confirm that for asymmetric vision, steady-state pressure varies with cone aperture and cannot be inferred from bulk measurements, demonstrating that torque-mediated reorientation fundamentally disrupts the equation of state in active matter.

5.2. Density-dependent propulsion

For confined quorum sensing particles (Fig. 8(a)), i.e., a speed reduction according to the local swimmer density as is the case for some bacteria, destroys the equation of state[35] (Fig. 8(c)). For active Brownian particles with quorum-sensing interactions, the propulsion speed $U(\bar{\rho})$ depends explicitly on the coarse-grained local density $\bar{\rho}(\boldsymbol{r})$. By applying Itô calculus to the density field $\psi(\boldsymbol{r},\theta)$, the mechanical pressure can be expressed in a microscopic form

$$P = \cdots + \frac{\zeta}{D_{\text{R}}}\int_0^\infty \mathrm{d}x\left\langle \partial_x U(\bar{\rho})\left[U(\bar{\rho})\frac{\hat{\rho}+\hat{m}_2}{2} - \frac{\hat{m}_1(\partial_x V)}{\zeta} - D_0\partial_x\hat{m}_1\right]\right\rangle, \tag{38}$$

where $\hat{m}_n$ denotes the nth angular moment of the microscopic distribution function, characterizing the orientational order of active particles at position $\boldsymbol{r}$. $\hat{m}_1$ measures the local polarization (the first orientational moment), and $\hat{m}_2$ represents nematic-like order. $\hat{\rho}$ represents the instantaneous local density at position $\boldsymbol{r}$. This exact expression shows that P is determined not only by bulk variables such as n_0 and the average propulsion speed, but also by spatial variations of $U(\bar{\rho})$ near boundaries, the density gradient $\partial_x U(\bar{\rho})$ and the external potential gradient $\partial_x V$. The coupling between motility and local density modifies the momentum flux at the walls, thereby breaking the equation of state in systems with density-dependent propulsion.

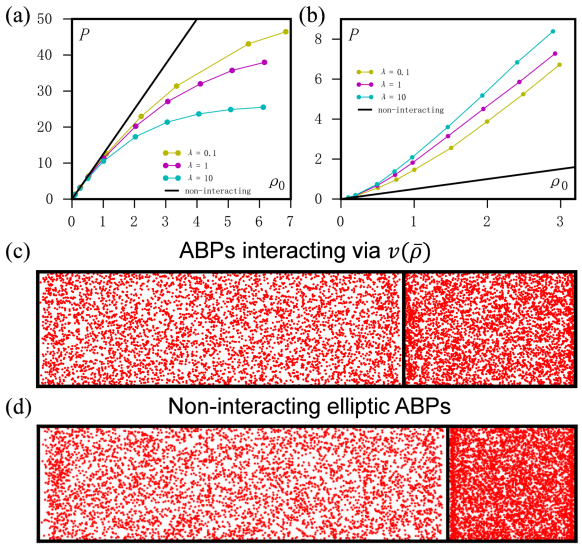


Fig. 8. Failure in the existence of an equation of state. (a)–(b) Pressure as a function of particle density in quorum-sensing and aligning ABPs, respectively. In the quorum-sensing system, the propulsion speed of particles decreases with the local density. The aligning system is composed of non-interacting elliptical ABPs. (c)–(d) Steady-state configurations of 10000 ABPs in a 200×50 cavity divided by a mobile asymmetric harmonic wall ($\lambda = 1$ on the left, $\lambda = 4$ on the right, where λ denotes the stiffness of the asymmetric harmonic wall). A spontaneous compression of the right half of the system indicates that the measured pressure depends on wall properties and that no well-defined equation of state exists for this system. Reused with permission from Ref. [35]. Copyright (2015) by the Springer Nature.

It is worth noting that, unlike the U_ϕ discussed in Subsection 3.1.1 which reflects the microscopic statistical configuration of the system but is not itself a measure of environmental sensing or interaction. In contrast, quorum sensing is an interaction mechanism widely observed in biological and active matter systems, in which particles detect and respond to local density via chemical signaling. This process modifies dynamical parameters such as propulsion speed $U(\bar{\rho})$ or rotational diffusivity $D_{\mathrm{R}}(\rho)$, thereby indirectly affecting swim pressure.

5.3. Boundary-induced effects

5.3.1. Stiffness of the boundary

Boundary dependence of the effective active pressure can be further emphasized[91] by demonstrating that the stiffness of the confining wall affects the measured active pressure. In their model, particles interacting with soft versus stiff walls produce distinct steady-state pressures, even when bulk properties remain unchanged (Fig. 9(a)). Wall deformation changes the local wall normal, altering particle–boundary momentum exchange. For anisotropic particles this acts as an external torque, while for spherical particles it induces reorientation through geometry, leading in both cases to a wall-stiffness dependence of active pressure.

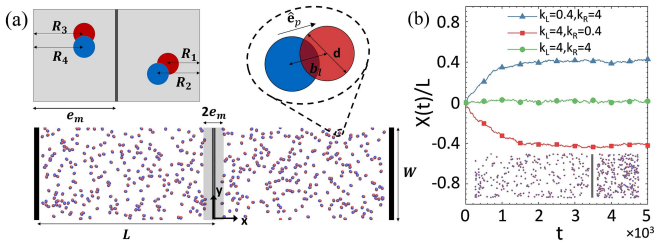


Fig. 9. Effect of wall stiffness on the motion of a mobile partition in active dumbbell systems. (a) Simulation box confined by two fixed walls in the x direction with a mobile wall separating dumbbells into two compartments. (b) The time evolution of the mobile wall position was tracked under three wall stiffness combinations. Shown inset is the final configuration for $k_{\mathrm{L}} = 0.4$ and $k_{\mathrm{R}} = 4$. Results were averaged over five runs with different initial dumbbell distributions. Reproduced from Ref. [91] (2021) under Creative Commons CC BY 4.0 license.

As shown in the figure, different wall stiffness values alter displacement of the wall accordingly (Fig. 9(b)). This behavior confirms that the measured pressure is not determined solely by bulk variables and that boundary mechanics can play an important role in stress generation. Their results provide direct evidence that, in active systems, the coupling between particle dynamics and boundary properties constitutes a genuine mechanism for the breakdown of the equation of state.

5.3.2. Alignment interaction between particle and wall

If torque is present when particles interact with boundaries, the pressure becomes boundary-dependent,[93] and the EOS fails.[40] This is clearly demonstrated by simulations of active elliptical particles confined in two chambers,[35] shown in Fig. 8(d). Specifically, the effective pressure in a noninteracting Brownian active particle system confined by two walls along the x-direction exerting forces $-\nabla V(x)$ with a wall potential $V(x)$ can be expressed as

$$P = \frac{nU_0^2\zeta\tau_{\mathrm{R}}}{2} - \frac{U_0\zeta_{\mathrm{R}}\tau_{\mathrm{R}}}{\zeta}\int \mathrm{d}x \int \mathrm{d}\theta \Gamma(x,\theta)\sin\theta\mathcal{P}(x,\theta), \quad (39)$$

where ζ_{R} is the rotational friction coefficient, $P(x,\theta)$ is the probability distribution of finding a particle at distance x from the wall and angle θ to the wall.

The $\Gamma(x,\theta)$ is an external torque, e.g., in order to model wall alignment of bacteria.[35] It becomes obvious now that if $\Gamma(x,\theta) = 0$, the active swim pressure given earlier is recovered. However, if $\Gamma(x,\theta) \neq 0$, the pressure explicitly depends on the wall potential and thus an equation of state is violated. More intuitively, for non-interacting elliptical ABPs

(with torque present) (Fig. 8(d)) and aligning ABPs (Fig. 8(b)), the concept of an EOS fails.

Further, Marc Joyeux *et al.*[90] extend this perspective by analyzing underdamped self-propelled dumbbells confined in a two-dimensional chamber separated by a mobile wall. This model incorporates finite inertia and breaks the torque-free condition due to the asymmetric geometry of the dumbbells. The dumbbells exert asymmetric pressure on the mobile wall, causing it to shift from the center. In the overdamped limit, this displacement vanishes and the pressure distribution becomes symmetric. However, in the low-damping regime, the pressure response becomes more intricate and even exhibits non-monotonic behavior with respect to the damping coefficient. At low density and weak damping, resonant recollisions of high-angular-momentum particles near the wall lead to oscillatory pressure variations, which cannot be captured by an effective equation of state.

5.3.3. Boundary geometry

In the strong confinement limit, where the container size is smaller than the particle persistence length, active particles are almost entirely localized at the boundary, and their density and pressure profiles are directly dictated by the boundary geometry.[94,95] For smooth convex boundaries, the steady-state density is proportional to the local curvature, leading to pronounced accumulation in high-curvature regions. Based on these findings, many simulations avoid such corner-trapping effects by choosing confinement geometries with rounded corners when setting up the simulation box.[90,96]

In polygonal geometries, where curvature is zero along edges and infinite at corners, particles become trapped at corners, producing sharp density peaks whose magnitude scales with the corner opening angle, while edges host almost no particles.[39] Although the theory is quantitatively most accurate for smoothly curved boundaries, it nonetheless qualitatively captures both the corner-trapping effect and the overall curvature dependence across a broad range of parameters.[97] These results highlight that tailoring the curvature distribution of the confining boundary provides a direct route to control density and pressure patterns in active systems.[93,94]

Taken together, these studies outline a coherent understanding of the conditions under which the equation of state fails in active systems. Factors such as torque arising from particle reorientation, interactions with structured boundaries, or external fields can disrupt the state function character of pressure. Similarly, density-dependent motility and collision-induced slow-down modify momentum transport in ways that are absent in equilibrium fluids, further undermining the applicability of a universal equation of state. The specific form of this breakdown is determined by the origin of torque, the density dependence of propulsion, the nature of particle dynamics (run-and-tumble or Brownian), and the imposed boundary conditions. Recognizing the interplay among these mechanisms is essential for capturing the diversity of active pressure phenomena and for assessing the prospects of a general thermodynamic framework for active matter.

5.3.4. Experimental evidence of boundary effect

To measure the pressure in active matter systems, Junot and his colleagues placed self-propelled and passive isotropic disks on a two-dimensional vibrated plate, with a deformable chain consisting of jointed beads (acting as a membrane) separating the two sides. As the disks move, they exert forces on the chain, causing measurable deformations, which serve as a proxy for mechanical pressure (see Fig. 10).

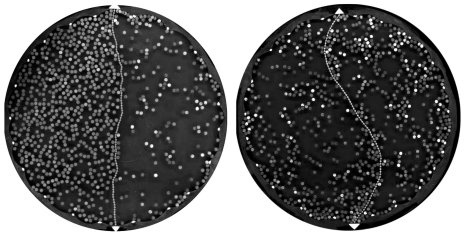


Fig. 10. Mechanical response of an active–passive mixture across a flexible membrane. Left: Stable configuration with more passive particles on the left balancing fewer active disks on the right. Right: Membrane deformation under equal partitioning of active disks, indicating mechanical instability. Reused with permission from Ref. [98]. Copyright (2017) by the American Physical Society.

In one of the configurations, passive and active disks were placed on opposite sides of the chain. By adjusting the number of disks on each side, the stresses exerted on the two sides of the membrane can be balanced such that the effective pressure on both sides is equal, indicated by the chain aligning into a straight line. However, replacing the chain with a different dynamical response, such as changing the bead size, the given balance is broken, which requires to readjust the densities on both sides, demonstrating the sensitivity of active pressure to the probe's microscopic features. When both sides contained self-propelled disks, mechanical equilibrium could only be achieved under specific conditions — when the number of disks on both sides was equal — resulting in an S-shaped chain. In all other configurations, the measured pressure was found to be dependent on the chain's dynamic properties, such as its relaxation time and responsiveness to particle collisions.

Although the chain-particle interactions in Ref. [98] are torque-free by construction, the S-shaped membrane instability does not necessarily imply torque-induced pressure differences. Instead, it may arise from curvature-dependent particle accumulation, similar to the wall curvature effects discussed in Ref. [94]. Meanwhile, for vibration-driven polar disks, the propulsive force is coupled with their orientational dynamics, which also contributes to the failure of EOS in this experiment.

Note that the experiment does not directly measure the bulk pressure, nor does it confirm its equivalence to the mechanical wall pressure. This result does not harm the concept

of an equation of state for active matter with pressure as a state variable, but shows that this effective pressure does not necessarily equal the average wall force. This represents a significant research gap, calling for new experimental designs that can simultaneously access both bulk and boundary pressure in active matter systems.

6. Summary and perspective

This review has presented a comprehensive summary of recent theoretical and experimental progress in understanding active pressure, with particular emphasis on active Brownian particles. From the definition of swim stress in dilute suspensions to the breakdown of the equation of state in systems dominated by torques or inertial effects, we have discussed the current understanding of how nonequilibrium momentum flux translates into mechanical pressure. While significant advances have been made in elucidating microscopic mechanisms such as confinement effects, interparticle interactions, and boundary influences, general principles governing active pressure remain elusive.

Several key questions are yet to be fully resolved. For instance, to what extent can pressure in active systems be treated as a state function? Is it possible to develop a unified theoretical framework that reconciles boundary-sensitive pressures observed experimentally with bulk momentum flux-based descriptions from simulations? Recent studies suggest that the local pressure in active systems should exclude the swim pressure, with the self-propulsion force regarded as an external force generated by the surrounding environment.[57,89,99,100] Sun *et al.*[101] recently established a more general intrinsic pressure framework and showed that it can recover mechanical equilibrium even in complex dry active systems with alignment, quorum sensing, and communication, which could potentially help for a unified mechanical description of active matter.

Additionally, the roles of torque interactions and boundary geometry in disrupting or preserving an equation of state continue to be actively investigated, particularly in systems with inhomogeneous particle accumulation or phase coexistence.[5,35,40,73–75,90,91] Experimental challenges further complicate this issue, as the measurement of swim pressure is often obscured by thermal noise[28,56] or influenced by the specific properties of measurement techniques, hindering direct comparisons between theory and experiments.

A yet different kind of effective pressure resulting from activity is observed in chiral active systems, i.e., systems consisting of active units showing not translational, but rotational motion in a common direction.[102] Therein, an effective pressure arises, which is proportional to a transport coefficient peculiar to chiral active systems called odd viscosity. The pressure points in the direction of emergent vorticity gradients, leading to correlations between vorticity and density.[103] To what extent this effective pressure bears similarities to the active pressure concept presented in this review is still an open question.

Despite these complexities, active pressure has demonstrated considerable potential for practical applications. Recent studies have shown that active pressure is more than an abstract theoretical concept, which can also be a functional and controllable mechanical resource. Examples range from enabling directed cargo transport via topological edge currents to harnessing nonequilibrium stress fluctuations for energy conversion in microscale engines.[104] Looking forward, establishing clearer connections among local stress distributions, particle-level interactions, and collective emergent behaviors will be critical for fully realizing the technological potential of active pressure in areas such as soft robotics, synthetic materials design, and bio-inspired micromachines.

Acknowledgements

Y.G. acknowledges financial support from the General Program of the National Natural Science Foundation of China (Grant No. 12474195), the Key Project of Guangdong Provincial Department of Education (Grant No. 2023ZDZX3021), and the Natural Science Foundation of Guangdong Province (Grant No. 2024A1515011343).

References

[1] Ji F, Wu Y, Pumera M and Zhang L 2023 *Adv. Mater.* **35** 2203959
[2] Illien P, Golestanian R and Sen A 2017 *Chem. Soc. Rev.* **46** 5508
[3] Cavagna A and Giardina I 2014 *Annual Review of Condensed Matter Physics* **5** 183
[4] Ramaswamy S 2010 *Annual Review of Condensed Matter Physics* **1** 323
[5] Cates M E and Tailleur J 2015 *Annual Review of Condensed Matter Physics* **6** 219
[6] Fruchart M, Hanai R, Littlewood P B and Vitelli V 2021 *Nature* **592** 363
[7] Mallory S A, Valeriani C and Cacciuto A 2018 *Annual Review of Physical Chemistry* **69** 59
[8] Huang Y, Wu C, Chen J and Tang J 2024 *Angewandte Chemie* **63** e202313885
[9] Yu N, Shah Z H, Yang M and Gao Y 2024 *Research* **7** 0304
[10] Elgeti J, Winkler R G and Gompper G 2015 *Reports on Progress in Physics* **78** 056601
[11] Mecke J, Nketsiah J O, Li R and Gao Y 2024 *Natl. Sci. Open* **3** 20230086
[12] Bechinger C, Di Leonardo R, Löwen H, Reichhardt C, Volpe G and Volpe G 2016 *Rev. Mod. Phys.* **88** 045006
[13] Dombrowski C, Cisneros L, Chatkaew S, Goldstein R E and Kessler J O 2004 *Phys. Rev. Lett.* **93** 098103
[14] Kemkemer R, Kling D, Kaufmann D and Gruler H 2000 *Euro. Phys. J. E* **1** 215
[15] Ballerini M, Cabibbo N, Candelier R, Cavagna A, Cisbani E, Giardina I, Lecomte V, Orlandi A, Parisi G, Procaccini A, Viale M and Zdravkovic V 2008 *Proc. Natl. Acad. Sci. USA* **105** 1232
[16] Makris N C, Ratilal P, Jagannathan S, Gong Z, Andrews M, Bertsatos I, Godø O R, Nero R W and Jech J M 2009 *Science* **323** 1734
[17] Marchetti M C, Joanny J F, Ramaswamy S, Liverpool T B, Prost J, Rao M and Simha R A 2013 *Rev. Mod. Phys.* **85** 1143
[18] Partridge B L, Johansson J and Kalish J 1983 *Environmental Biology of Fishes* **9** 253

[19] Vicsek T, Czirók A, Ben-Jacob E, Cohen I and Shochet O 1995 *Phys. Rev. Lett.* **75** 1226
[20] Anderson C, Theraulaz G and Deneubourg J L 2002 *Insectes Sociaux* **49** 99
[21] Gu F, Guiselin B, Bain N, Zuriguel I and Bartolo D 2025 *Nature* **638** 112
[22] Ning L, Zhu H, Yang J, Zhang Q, Liu P, Ni R and Zheng N 2024 *National Science Open* **3** 1
[23] Zhang J, Luijten E, Grzybowski B A and Granick S 2017 *Chem. Soc. Rev.* **46** 5551
[24] Aditi Simha R and Ramaswamy S 2002 *Phys. Rev. Lett.* **89** 058101
[25] Saintillan D and Shelley M J 2013 *Comptes Rendus Physique* **14** 497
[26] Saintillan D and Shelley M J 2008 *Phys. Rev. Lett.* **100** 178103
[27] Doostmohammadi A, Ignés-Mullol J, Yeomans J M and Sagués F 2018 *Nat. Commun.* **9** 3246
[28] Takatori S C, Yan W and Brady J F 2014 *Phys. Rev. Lett.* **113** 028103
[29] Foss D R and Brady J F 2000 *Journal of Rheology* **44** 629
[30] Mecke J, Gao Y, Ramírez Medina C A, Aarts D G A L, Gompper G and Ripoll M 2023 *Communications Physics* **6** 324
[31] Bricard A, Caussin J B, Desreumaux N, Dauchot O and Bartolo D 2013 *Nature* **503** 95
[32] Hall K R 1972 *The Journal of Chemical Physics* **57** 2252
[33] Phan S E, Russel W B, Cheng Z, Zhu J, Chaikin P M, Dunsmuir J H and Ottewill R H 1996 *Phys. Rev. E* **54** 6633
[34] Carnahan N F and Starling K E 1969 *The Journal of Chemical Physics* **51** 635
[35] Solon A P, Fily Y, Baskaran A, Cates M E, Kafri Y, Kardar M and Tailleur J 2015 *Nat. Phys.* **11** 673
[36] Mallory S A, Šarić A, Valeriani C and Cacciuto A 2014 *Phys. Rev. E* **89** 052303
[37] Yang X, Manning M L and Marchetti M C 2014 *Soft Matter* **10** 6477
[38] Ezhilan B, Alonso-Matilla R and Saintillan D 2015 *Journal of Fluid Mechanics* **781** R4
[39] Kaiser A, Wensink R and Löwen H 2012 *Phys. Rev. Lett.* **108** 268307
[40] Jin K and Jing G Y 2019 *Acta Phys. Sin.* **68** 170501 (in Chinese)
[41] Rands S 2011 *Applied Animal Behaviour Science* **134** 83
[42] Takatori S and Brady J 2016 *Current Opinion in Colloid & Interface Science* **21** 24
[43] Toner J, Tu Y and Ramaswamy S 2005 *Annals of Physics* **318** 170
[44] Yu N, Shah Z H, Basharat M, Wang S, Zhou X, Lin G, Edwards S A, Yang M and Gao Y 2023 *Soft Matter* **19** 9505
[45] Sokolov A, Apodaca M M, Grzybowski B A and Aranson I S 2010 *Proc. Natl. Acad. Sci. USA* **107** 969
[46] Dushman S 1938 *Journal of Chemical Education* **15** 550
[47] Quimby S L 1950 *Science* **112** 95
[48] Brady J F 1993 *The Journal of Chemical Physics* **98** 3335
[49] Reif F and Scott H L 1998 *American Journal of Physics* **66** 164
[50] Landau L and Lifshitz E 2013 *Fluid Mechanics: Landau and Lifshitz: Course of Theoretical Physics* **1** 1
[51] Truesdell C and Noll W 1965 *The Non-Linear Field Theories of Mechanics*, Flügge S ed. (Berlin: Springer) pp. 1–579
[52] Solon A P, Stenhammar J, Wittkowski R, Kardar M, Kafri Y, Cates M E and Tailleur J 2015 *Phys. Rev. Lett.* **114** 198301
[53] Winkler R G, Wysocki A and Gompper G 2015 *Soft Matter* **11** 6680
[54] Marini Bettolo Marconi U, Maggi C and Paoluzzi M 2017 *The Journal of Chemical Physics* **147** 024903
[55] Ginot F, Theurkauff I, Detcheverry F, Ybert C and Cottin-Bizonne C 2018 *Nat. Commun.* **9** 696
[56] Ginot F, Theurkauff I, Levis D, Ybert C, Bocquet L, Berthier L and Cottin-Bizonne C 2015 *Phys. Rev. X* **5** 011004
[57] Speck T and Jack R L 2016 *Phys. Rev. E* **93** 062605
[58] Romanczuk P, Bär M, Ebeling W, Lindner B and Schimansky-Geier L 2012 *Eur. Phys. J. Spec. Top.* **202** 1
[59] Irving J H and Kirkwood J G 1950 *The Journal of Chemical Physics* **18** 817
[60] Levis D, Codina J and Pagonabarraga I 2017 *Soft Matter* **13** 8113
[61] Falasco G, Baldovin F, Kroy K and Baiesi M 2016 *New J. Phys.* **18** 093043
[62] Cates M E and Tailleur J 2013 *Europhys. Lett.* **101** 20010
[63] Doi M 2013 *Soft Matter Physics* **2** 13
[64] Loi D, Mossa S and Cugliandolo L F 2008 *Phys. Rev. E* **77** 051111
[65] Jamali T 2020 *Active-Passive Brownian Particle in Two Dimensions*
[66] Lindner B and Nicola E 2008 *Euro. Phys. J. Spec. Top.* **157** 43
[67] Palacci J, Cottin-Bizonne C, Ybert C and Bocquet L 2010 *Phys. Rev. Lett.* **105** 088304
[68] Baek Y, Solon A P, Xu X, Nikola N and Kafri Y 2018 *Phys. Rev. Lett.* **120** 058002
[69] Takatori S C, De Dier R, Vermant J and Brady J F 2016 *Nat. Commun.* **7** 10694
[70] Golestanian R, Liverpool T B and Ajdari A 2007 *New J. Phys.* **9** 126
[71] Baxter R J 1968 *The Journal of Chemical Physics* **49** 2770
[72] Post A J and Glandt E D 1986 *The Journal of Chemical Physics* **84** 4585
[73] Caporusso C, Cugliandolo L, Digregorio P, Gonnella G and Suma A 2024 *Soft Matter* **20** 4208
[74] Fily Y and Marchetti M C 2012 *Phys. Rev. Lett.* **108** 235702
[75] Redner G S, Hagan M F and Baskaran A 2013 *Phys. Rev. Lett.* **110** 055701
[76] Schnitzer M J 1993 *Phys. Rev. E* **48** 2553
[77] Speck T, Bialké J, Menzel A and Löwen H 2013 *Phys. Rev. Lett.* **112** 238301
[78] Tailleur J and Cates M E 2008 *Phys. Rev. Lett.* **100** 218103
[79] Abaurrea Velasco C, Abkenar M, Gompper G and Auth T 2018 *Phys. Rev. E* **98** 022605
[80] Bäuerle T, Fischer A, Speck T and Bechinger C 2018 *Nat. Commun.* **9** 3232
[81] Fischer A, Schmid F and Speck T 2020 *Phys. Rev. E* **101** 012601
[82] Ridgway W J M, Dalwadi M P, Pearce P and Chapman S J 2023 *Phys. Rev. Lett.* **131** 228302
[83] Solon A P, Stenhammar J, Cates M E, Kafri Y and Tailleur J 2018 *Phys. Rev. E* **97** 020602
[84] Bialké J, Löwen H and Speck T 2013 *Europhys. Lett.* **103** 30008
[85] Bialké J, Siebert J T, Löwen H and Speck 2015 *Phys. Rev. Lett.* **115** 098301
[86] Caprini L and Marini Bettolo Marconi U 2021 *The Journal of Chemical Physics* **154** 024902
[87] Takatori S C and Brady J F 2017 *Phys. Rev. Fluids* **2** 094305
[88] Das S, Gompper G and Winkler R G 2019 *Scientific Reports* **9** 6608
[89] Steffenoni S, Falasco G and Kroy K 2017 *Phys. Rev. E* **95** 052142
[90] Joyeux M and Bertin E 2016 *Phys. Rev. E* **93** 032605
[91] Pirhadi E, Cheng X and Yong X 2021 *Scientific Reports* **11** 22204
[92] Lavergne F A, Wendehenne H, Bäuerle T and Bechinger C 2019 *Science* **364** 70
[93] Caprini L and Marconi U 2018 *Soft Matter* **14** 9044
[94] Fily Y, Baskaran A and Hagan M F 2014 *Soft Matter* **10** 5609
[95] Nikola N, Solon A P, Kafri Y, Kardar M, Tailleur J and Voituriez R 2016 *Phys. Rev. Lett.* **117** 098001
[96] Khatami M, Wolff K, Pohl O, Ejtehadi M R and Stark H 2016 *Scientific Reports* **6** 37670
[97] Fily Y, Baskaran A and Hagan M F 2015 *Phys. Rev. E* **91** 012125
[98] Junot G, Briand G, Ledesma-Alonso R and Dauchot O 2017 *Phys. Rev. Lett.* **119** 028002
[99] Yan W and Brady J F 2015 *Soft Matter* **11** 6235
[100] Speck T 2020 *Soft Matter* **16** 2652
[101] Sun Z, Li L, Wang C, Wang J, Chen H, Wang G, Liu L, Ye F and Yang M 2025 *Intrinsic pressure as a convenient mechanical framework for dry active matter*
[102] Banerjee D, Souslov A, Abanov A G and Vitelli V 2017 *Nat. Commun.* **8** 1573
[103] Mecke J, Gao Y, Ramírez Medina C A, Aarts D G A L, Gompper G and Ripoll M 2023 *Commun. Phys.* **6** 324
[104] Fodor É and Cates M E 2021 *Europhys. Lett.* **134** 10003